



Published in final edited form as:

Cell. 2013 July 3; 154(1): 75–88. doi:10.1016/j.cell.2013.05.060.

Presynaptic Neurexin-3 Alternative Splicing Trans-Synaptically Controls Postsynaptic AMPA-Receptor Trafficking

Jason Aoto^{1,2}, David C. Martinelli^{1,2}, Robert C. Malenka³, Katsuhiko Tabuchi^{1,2,4}, and Thomas C. Südhof^{1,2,*}

¹Dept. of Molecular and Cellular Physiology, Stanford University Medical School, 265 Campus Drive, CA 94305-5453, USA

²Howard Hughes Medical Institute, Stanford University Medical School, 265 Campus Drive, CA 94305-5453, USA

³Dept. of Psychiatry, Nancy Pritzker Laboratory, Stanford University Medical School, 265 Campus Drive, CA 94305-5453, USA

⁴Dept. of Neurophysiology, Shinshu University School of Medicine, Matsumoto 390-8621 Japan

Abstract

Neurexins are essential presynaptic cell-adhesion molecules that are linked to schizophrenia and autism, and are subject to extensive alternative splicing. Here, we used a novel genetic approach to test the physiological significance of neurexin alternative splicing. We generated knock-in mice in which alternatively spliced sequence #4 (SS4) of neurexin-3 is constitutively included, but can be selectively excised by cre-recombination. SS4 of neurexin-3 was chosen because it is highly regulated and controls neurexin-binding to neuroligins, LRRTMs, and other ligands. Unexpectedly, constitutive inclusion of SS4 in presynaptic neurexin-3 decreased postsynaptic AMPA- but not NMDA-receptor levels and enhanced postsynaptic AMPA-receptor endocytosis. Moreover, constitutive inclusion of SS4 in presynaptic neurexin-3 abrogated postsynaptic AMPA-receptor recruitment during NMDA-receptor-dependent LTP. These phenotypes were fully rescued by constitutive excision of SS4 in neurexin-3. Thus, alternative splicing of presynaptic neurexin-3 controls postsynaptic AMPA-receptor trafficking, revealing an unanticipated alternative splicing mechanism for trans-synaptic regulation of synaptic strength and long-term plasticity.

Introduction

Central synapses exhibit a large diversity in properties, such as presynaptic release probability, postsynaptic receptor composition, and long-term plasticity. In a given neuron, these properties depend on both the pre- and the postsynaptic neuron (Reyes et al., 1998; Koester and Johnston, 2005). Trans-synaptic cell-adhesion molecules not only organize and synchronize assembly of synapses, but likely also determine their properties and diversity. Neurexins are trans-synaptic cell-adhesion molecules that are candidate molecules for

© 2013 Elsevier Inc. All rights reserved.

*Address for correspondence at tcs1@stanford.edu.

Publisher's Disclaimer: This is a PDF file of an unedited manuscript that has been accepted for publication. As a service to our customers we are providing this early version of the manuscript. The manuscript will undergo copyediting, typesetting, and review of the resulting proof before it is published in its final citable form. Please note that during the production process errors may be discovered which could affect the content, and all legal disclaimers that apply to the journal pertain.

mediating trans-synaptic specification of synaptic properties (Craig and Kang, 2007; Südhof, 2008; Krueger et al., 2012).

Neurexins are expressed as α - and β -neurexins from independent promoters in three genes (Ushkaryov et al., 1992 and 1994; Ushkaryov and Südhof, 1993; Tabuchi and Südhof, 2002; Rowen et al., 2002). The larger α -neurexins are composed of 6 LNS-domains with 3 interspersed EGF-like domains followed by a transmembrane region and a short cytoplasmic tail. The smaller β -neurexins lack the N-terminal 5 LNS and 3 EGF-like domains of α -neurexins, but instead contain a unique short N-terminal sequence. β -Neurexins splice into the 6th LNS-domain of α -neurexins, and are identical with α -neurexins in all C-terminal sequences. The six principal neurexins (Nrx1 α -3 α and Nrx1 β -3 β) are expressed in differential but overlapping patterns in all neurons, such that most neurons synthesize multiple α - and β -neurexins in different combinations (Ullrich et al., 1995).

In mice, triple knockout (KO) of Nrx1 α , Nrx2 α , and Nrx3 α is lethal despite continued expression of Nrx1 β , Nrx2 β , and Nrx3 β (Missler et al. 2003). α -Neurexin triple KO mice die because of a severe impairment in synaptic transmission. Neurexins are assumed to be presynaptic because they act as α -latrotoxin receptors (Ushkaryov et al., 1992; Sugita et al., 1999), and because the α -neurexin triple KO phenotype suggested a presynaptic function (Missler et al., 2003). However, triple α -neurexin KO mice also displayed a postsynaptic phenotype (Kattenstroth et al., 2004), and recent studies in *Drosophila* and *C. elegans* proposed a postsynaptic localization for neurexins (Chen et al., 2012; Hu et al., 2012). These results are consistent with at least some (Taniguchi et al., 2007) but not all immunolocalization data (Ushkaryov et al., 1992), making it uncertain whether neurexins act pre- or postsynaptically.

Mutations in the human Nrx1 (*NRXN1*) and Nrx2 (*NRXN2*) gene have been associated with diverse neuropsychiatric disorders, especially autism and schizophrenia (reviewed in Südhof, 2008; Reichelt et al., 2012). Changes in the human Nrx3 gene (*NRXN3*) have also been associated with autism (Vaags et al., 2012), and additionally linked to drug addiction and obesity (Hishimoto et al., 2007; Lachman et al., 2007; Heard-Costa et al., 2009).

Neurexins are alternatively spliced at 5 canonical sites (referred to as splice sites 1-5 [SS1-SS5]; (Ullrich et al., 1995)). SS1, SS2, and SS3 are specific to α -neurexins, while SS4 and SS5 are present in both α - and β -neurexins. Neurexin alternative splicing is highly regulated. In particular, neurexin SS4 splice variants are differentially expressed in various brain regions (Ullrich et al., 1995), exhibit a diurnal cycle (Shapiro-Reznik et al., 2012), and are modulated by neuronal activity (Resnick et al., 2008; Iijima et al., 2011; Rozic et al., 2012). These data suggest that neurexin alternative splicing may be physiologically important, but its biological significance has not been tested.

Neurexins bind to multiple postsynaptic cell-adhesion molecules, including neuroligins (Ichtchenko et al., 1995), dystroglycan (Sugita et al., 2001), LRRTMs (Ko et al., 2009; de Wit et al., 2009; Siddiqui et al., 2010), GluR62 via cerebellins (Uemura et al., 2010), and CIRL/latrophilin (Boucard et al., 2012). Binding of these ligands is modulated by neurexin alternative splicing at SS4. SS4 exists in two forms that include (SS4+) or exclude (SS4-) an alternatively spliced exon encoding 30 residues. Strikingly, only SS4- neurexins bind to dystroglycan, CIRL/latrophilin, and LRRTMs (Boucard et al., 2012; Ko et al., 2009; Siddiqui et al., 2010; Sugita et al., 2001), while only SS4+ neurexins bind to cerebellins (Matsuda and Yuzaki, 2011; Uemura et al., 2010). Moreover, SS4- and SS4+ neurexins exhibit distinct affinities for different isoforms of neuroligins, creating a 'splice code' of interactions (Boucard et al., 2005; Chih et al., 2006; Comoletti et al., 2006). However, despite the known effect of SS4 alternative splicing on neurexin-ligand interactions and its

mechanistic understanding, it is unclear whether SS4 alternative splicing is physiologically important. No approaches are available to directly test the significance of alternative splicing for molecules such as neurexins, which are alternatively processed at multiple positions and whose overexpression in itself may produce biological effects. Apart from the fact that no KOs targeting both α - and β -neurexins are available, such studies are made difficult because rescue experiments cannot test all splice combinations at physiological expression levels.

Here, we apply a novel approach to test the biological significance of neurexin alternative splicing at SS4. Using homologous recombination, we changed the splice-acceptor sequence of the alternatively spliced SS4 exon, thereby converting it into a constitutively included exon that is no longer subject to alternative splicing. At the same time, we rendered the SS4 exon conditional by floxing it. To the best of our knowledge, this genetic manipulation is the first instance where alternative splicing of a vertebrate gene is controlled genetically in a conditional manner. Using this approach, we found that constitutive expression of *Nrx3*-SS4+ produced a selective decrease in postsynaptic AMPA-receptor (AMPA) but not NMDA-receptor (NMDAR) trafficking, such that synaptic strength was decreased and NMDAR-dependent LTP was attenuated. This phenotype was fully reversed by cre-dependent excision of the SS4 exon. Moreover, we found that the effect of SS4 alternative splicing was not mediated by a cell-autonomous postsynaptic effect, but by a trans-synaptic non-cell-autonomous action of presynaptic *Nrx3* on postsynaptic neurons, and that constitutive expression of *Nrx3*-SS4+ causes a loss of the postsynaptic neurexin ligand LRRTM2. These results provide the first test of the physiological function of neurexin alternative splicing *in vivo*, and demonstrate a novel mechanism by which alternative splicing of a neurexin in a presynaptic neuron trans-synaptically controls postsynaptic properties.

Results

Region-specific alternative splicing of *Nrx3* at SS4

Although qualitative studies showed that alternative splicing of neurexins at SS4 is highly regulated (Ullrich et al., 1995), no quantitative assessment of neurexin alternative splicing is available. Thus, we developed quantitative rt-PCR assays for the alternatively spliced versions of SS4 for *Nrx1*, *Nrx2*, and *Nrx3* (Fig. S1), and measured their mRNA levels in various brain regions from adult mice (Fig. 1A).

We found that the three neurexin genes were expressed at comparable levels in different brain regions, and exhibited a coordinate but differential pattern of SS4 alternative splicing (Fig. 1A). Some brain regions (e.g., striatum and cerebellum) expressed primarily (~90%) SS4+ forms of all three neurexins. Other brain regions (e.g., cortex and hippocampus) expressed similar amounts of SS4+ and SS4- forms of *Nrx1* and *Nrx2*, but primarily the SS4- form of *Nrx3* (~90%; Fig. 1A). Thus, alternative splicing of neurexins at SS4 is regionally regulated, with the largest differential in expression observed for *Nrx3*, prompting us to focus on this isoform.

Conditional mutant mice in which SS4 alternative splicing of *Nrx3* is blocked

To test the role of SS4 alternative splicing of *Nrx3*, we sought to develop a new genetic approach. We noted that the alternatively spliced SS4 exon in the mouse *Nrxn3* gene (exon 20; (Tabuchi and Südhof, 2002)) contains an unusual purine-rich splice acceptor sequence (Fig. 1B). Using homologous recombination in mouse embryonic stem cells, we converted this imperfect splice acceptor sequence into a canonical consensus sequence (Fig. 1B). We also introduced flanking loxP sites, such that exon 20 could be conditionally deleted. Using this strategy, we obtained mutant mice that were designed to constitutively insert the

normally alternatively spliced SS4 sequence into all *Nrx3* mRNAs, thus rendering all *Nrx3* mRNAs SS4+ (referred to as *Nrx3*^{SS4+} genotype). At the same time, these mutant mice allow exclusion of the SS4 sequence after cre-recombinase mediated deletion of exon 20, rendering all *Nrx3* mRNAs SS4- (referred to as *Nrx3*^{SS4-} genotype; Fig. 1B).

Homozygous *Nrx3*^{SS4+} and *Nrx3*^{SS4-} mice (obtained from *Nrx3*^{SS4+} mice by germline deletion of exon 20) were viable and fertile. To test the effectiveness of our genetic strategy, we cultured hippocampal neurons from newborn wild-type (WT) and *Nrx3*^{SS4+} mice. We infected WT neurons at DIV4-5 with lentivirus expressing GFP, and the *Nrx3*^{SS4+} neurons with lentiviruses expressing inactive or active cre-recombinase, thereby producing controlled sets of cultured WT, *Nrx3*^{SS4+}, and *Nrx3*^{SS4-} neurons. We then measured *Nrx3*-SS4+ and *Nrx3*-SS4- mRNA levels in all three sets of neurons at DIV14-16. We found that *Nrx3*^{SS4+} neurons expressed only *Nrx3*-SS4+ mRNAs as predicted, whereas *Nrx3*^{SS4-} neurons expressed only *Nrx3*-SS4- mRNAs (Fig. 1C). Total *Nrx3* mRNA levels were not significantly altered by either manipulation. Thus, we generated mutant mice in which neurons produce only *Nrx3*-SS4+ mRNAs, but can be converted by cre-recombination to produce only *Nrx3*-SS4- mRNAs.

Blocking SS4 alternative splicing of *Nrx3* alters AMPAR-mediated responses

Electrophysiological recordings revealed that spontaneous miniature excitatory postsynaptic currents (mEPSCs) exhibited a significantly lower amplitude in *Nrx3*^{SS4+} than in WT or *Nrx3*^{SS4-} neurons, but displayed no change in frequency (Figs. 1D, 1E, and S1C). Neither the amplitude nor the frequency of spontaneous miniature inhibitory postsynaptic currents (mIPSCs) was altered (Figs. 1D, 1F, and S1E). The mEPSC or mIPSC rise or decay kinetics and intrinsic properties of the neurons were unchanged (Figs. S1D and S1F). Neurexins are thought to be presynaptic, whereas changes in the mEPSC amplitude generally reflect postsynaptic changes. Thus, these findings were surprising and suggested that alternative splicing of presynaptic *Nrx3* may alter excitatory synaptic strength by a postsynaptic mechanism.

We next measured evoked excitatory postsynaptic currents (EPSCs) mediated by AMPARs and NMDARs, and inhibitory postsynaptic currents (IPSCs) mediated by GABA_A-receptors. We observed a large selective reduction (~45%) in AMPAR-mediated EPSCs in *Nrx3*^{SS4+} neurons compared to WT or *Nrx3*^{SS4-} neurons (Fig. 1G). We detected no change in NMDAR-mediated EPSCs or in IPSCs (Figs. 1H and 1I). Paired-pulse ratios (PPRs) of NMDAR EPSCs were identical in WT, *Nrx3*^{SS4+}, and *Nrx3*^{SS4-} neurons (Figure S1F). Together, these data suggest that SS4 alternative splicing selectively alters postsynaptic AMPAR responses without changing presynaptic neurotransmitter release or postsynaptic NMDAR responses.

SS4 alternative splicing of all neurexins controls postsynaptic AMPARs

We next asked whether the decrease in AMPAR-mediated EPSCs in *Nrx3*^{SS4+} neurons can be reversed by expression of different neurexins in an SS4-dependent manner. We superinfected WT, *Nrx3*^{SS4+}, and *Nrx3*^{SS4-} neurons at DIV4-5 with lentiviruses expressing either control GFP or 'rescue' neurexins, and measured evoked AMPAR-mediated EPSCs at DIV14-16 (Fig. 2).

We found that both *Nrx3*α-SS4- and *Nrx3*β-SS4- cDNAs rescued the decrease in AMPAR responses in *Nrx3*^{SS4+} neurons without affecting AMPAR responses in WT or *Nrx3*^{SS4-} neurons (Figs. 2A and 2B). In contrast, the *Nrx3*β-SS4+ cDNA did not rescue the decreased AMPAR responses in *Nrx3*^{SS4+} neurons. Moreover, we observed that *Nrx1*β-SS4- and *Nrx2*β-SS4- fully rescued the decreased AMPAR phenotype in *Nrx3*^{SS4+} neurons, whereas

Nrx1 β -SS4⁺ and Nrx2 β -SS4⁺ did not (Figs. 2C and 2D). Thus, alternative splicing of all neurexins at SS4 redundantly controls postsynaptic AMPAR responses.

***Nrx3*^{SS4+} decreases postsynaptic AMPAR levels and increases AMPAR endocytosis**

We labeled surface AMPARs in cultured WT, *Nrx3*^{SS4+}, and *Nrx3*^{SS4-} neurons with antibodies to the extracellular sequences of the AMPAR subunits GluA1 and GluA2. We fixed and permeabilized the GluA1-stained neurons and stained them for the intracellular presynaptic marker vGluT1 and the postsynaptic marker PSD95 (Fig. S2A). Quantification of surface GluA1- and GluA2-containing puncta or of intracellular vGluT1- or PSD95-containing puncta did not reveal a difference in synapse density between WT, *Nrx3*^{SS4+}, and *Nrx3*^{SS4-} neurons (Figs. 3A, 3B, and S2B; for absolute values, see Fig. S2C). However, the size of postsynaptic GluA1- and GluA2-containing surface clusters was 40-50% smaller in *Nrx3*^{SS4+} neurons than in WT and *Nrx3*^{SS4-} neurons, whereas the size of PSD95- or vGluT1-containing clusters was not significantly altered (Fig. 3B). The decrease in GluA1 and GluA2 puncta size was uniformly distributed among synapses (Fig. 3C). No effect on AMPAR intensity (i.e., the amount of AMPARs per area) was observed (Fig. S2B).

To determine why the *Nrx3*^{SS4+} genotype decreased postsynaptic AMPAR levels, we measured GluA1 internalization in cultured hippocampal neurons (Lin et al., 2000). We incubated WT, *Nrx3*^{SS4+}, and *Nrx3*^{SS4-} neurons briefly (5 min) with an antibody to the extracellular N-terminus of GluA1, followed by a 15 min chase (Fig. S2D). We then fixed the neurons without permeabilization, labeled them with an AlexaFluor488-tagged secondary antibody (green) to mark surface GluA1 receptors, permeabilized the neurons, and labeled them with a different secondary antibody that was AlexaFluor546-tagged (red) to detect internalized GluA1 receptors (Fig. 3D).

Strikingly, we found that GluA1 internalization was increased ~60% in *Nrx3*^{SS4+} neurons compared to WT and to *Nrx3*^{SS4-} neurons, which exhibited identical values (Fig. 3E). Taken together, these data show that the constitutive inclusion of SS4 in *Nrx3* decreases postsynaptic surface AMPARs and accelerates AMPAR endocytosis.

Presynaptic membrane-tethered *Nrx3* sequences control postsynaptic AMPARs

To test whether *Nrx3*-SS4⁻ acts pre- or postsynaptically to stabilize postsynaptic AMPARs, we sparsely transfected neurons. We then measured whether postsynaptically expressed *Nrx3*-SS4⁻ could rescue the decrease in AMPAR responses in *Nrx3*^{SS4+} neurons (Fig. 4A). We observed no difference between *Nrx3*^{SS4+} neurons without or with postsynaptic 'rescue' by *Nrx3*-SS4⁻, suggesting that postsynaptic *Nrx3* cannot stabilize postsynaptic AMPAR levels. To confirm this conclusion, we asked whether cre-recombinase mediated postsynaptic conversion of *Nrx3*^{SS4+} into *Nrx3*^{SS4-} rescues AMPAR levels in a neuron (Fig. 4B). Again, we failed to observe rescue, suggesting that postsynaptic *Nrx3* does not contribute to the regulation of postsynaptic AMPARs, and arguing by default that alternative splicing of *Nrx3* at SS4 must act by a presynaptic mechanism.

Does presynaptic *Nrx3* β -SS4⁻ stabilize AMPARs via an intra- or extracellular interaction? We addressed this question by testing a fusion protein composed of the extracellular *Nrx3* β sequences and the PDGF-receptor transmembrane region (Fig. 4C). Strikingly, this protein fully rescued the decreased AMPAR EPSCs in *Nrx3*^{SS4+} neurons, but only when SS4 was excised. This result shows that no intracellular *Nrx3* sequences are required for stabilizing AMPARs, but raises the interesting question whether naturally occurring secreted variants of *Nrx3* encoded by some inserts in SS5 which contain a stop codon might also rescue the *Nrx3*^{SS4+} phenotype. In other words, could *Nrx3*-SS4⁻ act as a paracrine factor? However, we found that secreted *Nrx3* β - independent of the SS4 splice variant - was unable to rescue

AMPA EPSCs in *Nrx3^{SS4+}* neurons, suggesting that membrane-tethering of the Nrx3 extracellular sequences is essential (Fig. 4D).

Nrx3-SS4 alternative splicing controls AMPAR responses *in vivo*

Although cultured neurons allow a quantitative definition of synaptic parameters such as synaptic strength, cultured neurons lack some properties of neural networks, such as a defined cytoarchitecture or long-term plasticity. Moreover, differentiation between pre- and postsynaptic effects can be difficult in cultured neurons. To address these issues, we analyzed the effects of Nrx3-SS4 alternative splicing in presynaptic CA1 neurons of the hippocampus at synapses formed onto postsynaptic pyramidal neurons in the subiculum (Fig. 5A). The subiculum is the major synaptic output for hippocampal CA1 neurons, but additionally receives synapses from the entorhinal, perirhinal, and prefrontal cortex (O'Mara, 2005). We decided to analyze the CA1-subiculum synapse because it is amenable to specifically presynaptic manipulations by stereotactic injection of viruses into the CA1 region (Xu et al., 2012). This approach allowed us to record from uninfected subicular neurons receiving inputs from infected CA1 neurons, and thus enabled us to selectively probe the effect of presynaptic alternative splicing of Nrx3 on postsynaptic AMPAR responses (Fig. 5A).

We stereotactically injected the hippocampal CA1 region of WT or *Nrx3^{SS4+}* mice at P21 with control or cre-recombinase expressing adeno-associated viruses (AAVs), and analyzed the mice at P35-42. EGFP expression documented that the CA1 region and dentate gyrus of the hippocampus, but not the subiculum or the CA3 region, were infected (Fig. 5A). Thus, the infected CA1 pyramidal neurons either exhibit a WT genotype, an *Nrx3^{SS4+}* genotype (control virus in *Nrx3^{SS4+}* mice, referred to as CA1^{Ctrl}), or an *Nrx3^{SS4-}* genotype (cre-expressing virus in *Nrx3^{SS4+}* mice, referred to as CA1^{Cre}). We sectioned horizontal slices (300 μ m) from the dorsal hippocampus of injected mice, stimulated CA1 axons with an extracellular electrode placed in the alveus/stratum oriens at the border of the CA1 pyramidal layer and the subiculum, and recorded from subicular pyramidal neurons (Fig. 5A).

We first measured the AMPAR to NMDAR ratio. Strikingly, the AMPAR/NMDAR ratio was significantly decreased in *Nrx3^{SS4+}*-CA1^{Ctrl} but not in *Nrx3^{SS4+}*-CA1^{Cre} neurons compared to WT controls (Fig. 5B). This result is consistent with a selective decrease in AMPAR but not NMDAR responses observed in cultured *Nrx3^{SS4+}* neurons, suggesting that Nrx3-SS4 alternative splicing bidirectionally and trans-synaptically regulates postsynaptic AMPAR responses *in vivo* (Figs. 1G and 1H).

To confirm that presynaptic Nrx3-SS4 alternative splicing regulates postsynaptic AMPARs, we measured AMPAR-mediated input-output curves. The subiculum contains two types of pyramidal neurons, regular and burst firing neurons. These neurons differ in firing patterns (Fig. S3A) and express different forms of LTP, but receive similar inputs and exhibit comparable basal transmission properties (Taube, 1993; Staff et al., 2000; Menendez de la Prida et al., 2003; Wozny et al., 2008). Both regular and burst firing subicular neurons displayed a significant decrease in AMPAR mediated synaptic responses in *Nrx3^{SS4+}*-CA1^{Ctrl} neurons compared to either WT or *Nrx3^{SS4+}*-CA1^{Cre} neurons, confirming a decrease in AMPAR mediated responses (Figs. 5C and 5E). We also measured paired-pulse ratios in regular and burst firing subicular neurons to identify possible presynaptic changes, but detected none (Figs. 5D, 5F, S3B, and S3C). Viewed together, these data indicate that in adult mice *in vivo*, constitutive inclusion of SS4 in presynaptic *Nrx3* mRNAs causes a selective and highly significant decrease in post-synaptic AMPAR responses that can be reversed by removal of the SS4 exon.

Constitutive presynaptic *Nrx3-SS4+* expression impairs postsynaptic LTP

In regular firing neurons of the subiculum, the threshold for LTP induction is high, and LTP is mediated by a postsynaptic, NMDAR-dependent mechanism similar to classical LTP at Schaffer-collateral CA1-region synapses of the hippocampus (Wozny et al., 2008). By contrast, in burst firing neurons, the LTP induction threshold is low, and LTP is mediated by a presynaptic mechanism that increases the probability of glutamate release. Although the mechanisms of LTP differ between the two types of neurons, LTP induction appears to require Ca^{2+} -influx via NMDA-receptors in both (Fig. S4; Wozny et al., 2008).

We induced LTP in acute slices from WT, *Nrx3^{SS4+}-CA1^{Ctrl}* and *Nrx3^{SS4+}-CA1^{Cre}* mice by four 100 Hz tetani separated by 10 s, and measured LTP-induction in regular and burst firing neurons. We observed a marked reduction (~70%) of LTP in regular firing neurons from *Nrx3^{SS4+}-CA1^{Ctrl}* mice compared to WT and *Nrx3^{SS4+}-CA1^{Cre}* mice (Figs. 6A and 6B). We detected no decrease in paired-pulse ratio after LTP induction in regular firing neurons in any genotype, in agreement with the finding that LTP in these neurons is postsynaptic (Figs. 6B, S4B, and S4C).

In contrast to regular firing neurons, we observed no significant difference in LTP in burst firing neurons in slices from *Nrx3^{SS4+}-CA1^{Ctrl}*, *Nrx3^{SS4+}-CA1^{Cre}*, and WT mice (Figs. 6C and D). Consistent with the previously described presynaptic mechanism of LTP in burst-firing neurons (Wozny et al., 2008), we found that LTP induction in burst firing neurons caused a significant decrease in the paired-pulse ratio in all three genotypes (Fig. 6D). Taken together, these data demonstrate that constitutive presynaptic expression of *Nrx3-SS4+* impairs postsynaptic LTP in regular firing neurons.

Constitutive *Nrx3-SS4+* expression decreases postsynaptic LRRTM2 levels

The reduction of AMPAR-mediated basal synaptic transmission and the block of LTP by presynaptic *Nrx3-SS4+* suggests that presynaptic *Nrx3-SS4+* may interact with one or several postsynaptic ligand(s) that control postsynaptic AMPAR levels. Two neurexin ligands are linked to AMPARs, neuroligins (Chubykin et al., 2007; Etherton et al., 2011) and LRRTMs (de Wit et al., 2009; Schwenk et al., 2012). Moreover, reduction of neuroligin and LRRTM levels in postsynaptic neurons specifically impaired AMPAR-mediated transmission in vivo (Soler-Llavina et al., 2011). Furthermore, we recently found that LRRTM knockdown in vivo severely impairs NMDAR-mediated LTP (Soler-Llavina et al., 2013). Thus, we tested whether the postsynaptic levels of LRRTM2 (the major LRRTM isoform in the hippocampus) and neuroligin-1 (the major neuroligin isoform of excitatory synapses) were altered by *Nrx3-SS4+* expression (Figs. 7A-7C and S5). Strikingly, we found that the apparent postsynaptic surface levels of LRRTM2 were decreased ~45%, whereas neuroligin-1 did not exhibit a significant change. These data support the notion that presynaptic *Nrx3-SS4+* acts to enable postsynaptic AMPAR retention by activating LRRTM2 and possibly other ligands.

Discussion

Alternative splicing of neurexins is highly regulated and controls neurexin binding to multiple ligands, but its biological significance is unknown. Using a novel genetic strategy, we here addressed this question. We focused on alternative splicing of *Nrx3* at SS4 which is particularly strongly regulated (Fig. 1A) and controls *Nrx3*-binding to neuroligins, LRRTMs, cerebellins, dystroglycan, and CIRL/latrophilin (Ichtchenko et al., 1995; Sugita et al., 2001; Ko et al., 2009; Siddiqui et al., 2010; Uemura et al., 2010; Boucard et al., 2012). Alternative splicing of *Nrx3* at SS4 involves inclusion or exclusion of a single exon that exhibits an unusual purine-rich splice acceptor sequence (Tabuchi and Südhof, 2002). We

converted this non-canonical splice-acceptor sequence into a canonical splice-acceptor sequence to render the exon constitutively 'spliced in', and flanked the SS4 exon with loxP sites to allow the exon to be constitutively 'spliced out' by cre recombinase (Figs. 1B and Fig. 1C). Different from traditional approaches, such as conditional knockout-and-rescue methods, this genetic approach does not alter expression of the endogenous gene and does not interfere with other alternative splicing events. The genetic approach we describe here enabled us to examine the role of neurexin alternative splicing *in vivo*, and may be generally applicable for studies of the physiological significance of alternative splicing.

Using the new genetic tool we generated, we demonstrate that alternative splicing of presynaptic Nr3 at SS4 trans-synaptically controls the strength of excitatory synapses by controlling postsynaptic AMPAR levels. To the best of our knowledge, this is the first description of trans-synaptic control of postsynaptic receptors by a presynaptic ligand. Moreover, although neurexin alternative splicing has been extensively studied *in vitro* (Ullrich et al., 1995; Resnick et al., 2008; Iijima et al., 2011), its significance was unknown. This is the first demonstration that alternative splicing of neurexins is physiologically important. In Nr3-SS4+ neurons, the number of synapses was unchanged, as evidenced by the lack of change in synapse density, mEPSC frequency, and NMDAR-mediated EPSCs. However, the synaptic levels of AMPARs were decreased, as evidenced by decreased GluA1 and GluA2 puncta sizes, decreased mEPSC amplitudes, decreased evoked AMPAR-mediated EPSCs, and increased AMPAR endocytosis (Figs. 1 and 3). Viewed together, these data suggest that presynaptic Nr3-SS4- but not Nr3-SS4+ produces anchoring sites for postsynaptic AMPARs (Fig. 7D).

In controlling postsynaptic AMPAR levels, neurexins act strictly presynaptically, as shown by the specifically pre- and postsynaptic manipulations we performed *in vitro* (Fig. 4) and *in vivo* (Figs. 5 and 6). Thus, our results offer a potential explanation for the observation that the properties of a synapse are determined by a trans-synaptic interaction between pre- and postsynaptic elements (Reyes et al., 1998; Koester and Johnston, 2005).

Our data also suggest a mechanism by which alternative splicing of presynaptic neurexins may control postsynaptic AMPAR content. Presynaptic membrane-tethered Nr3 was sufficient for stabilizing postsynaptic AMPARs, whereas secreted Nr3 was inactive (Fig. 4). Thus, presynaptic neurexins likely connect to a postsynaptic ligand. Neurexins interact with several postsynaptic ligands in a largely competitive manner, most importantly with neuroligins and LRRTMs (Fig. 7D). These interactions form a dynamic interaction network in which the postsynaptic neurexin ligands in turn interact with other ligands (e.g., see Lee et al., 2013). The relative concentrations and alternative splicing of neurexins and their ligands determine the state of the network. This dynamic interaction network results in a binding equilibrium whereby not a single neurexin binding reaction can explain all of the observed actions of neurexins, but the overall state of the network determines the properties of a synapse.

Among neurexin ligands, both neuroligins and LRRTMs regulate AMPARs (Chubykin et al., 2007; de Wit et al., 2009; Etherton et al., 2011; Soler-Llavina et al., 2011; Schnell et al., 2012). Strikingly, we found that postsynaptic LRRTM2 is decreased in Nr3-SS4+ neurons (Figs. 7A-7C). LRRTM2 binds only to SS4- neurexins (Ko et al., 2009; Siddiqui et al., 2010), suggesting that neurexins control AMPARs by binding to LRRTMs, although neuroligins may also contribute because they differentially interact with both SS4+ and SS4- neurexins (Ichtchenko et al., 1995; Boucard et al., 2005; Chih et al., 2006). Given the importance of SS4 in regulating ligand interactions of neurexins, it seems likely that SS4 is a central regulator of the neurexin-based dynamic protein-interaction network. Changing

alternative splicing of *Nrx3* at SS4 may shift this network without altering other neurexin functions, thereby producing the AMPAR phenotype we observed (Fig. 7D).

Finally, our study constitutes the first demonstration whereby a presynaptic change controls postsynaptic NMDAR-dependent LTP. Specifically, we show that alternative splicing of SS4 in *Nrx3* not only regulates constitutive AMPAR trafficking, but also enables activity-dependent recruitment of AMPARs during LTP induction (Fig. 6). The decades-old debate of the whether NMDAR-dependent LTP is pre- or postsynaptically induced was resolved when LTP was found to be induced by recruitment of AMPARs to synapses (Kerchner and Nicoll, 2008). Although LTP is clearly postsynaptically induced, our results show that LTP induction nevertheless requires presynaptic ‘permission’, thereby rendering LTP under control of both pre- and postsynaptic neurons (Fig. 6). This permission is likely mediated by *Nrx3*-binding to LRRTMs since LRRTM knockdowns also produce a decrease in LTP (Soler-Llavina et al., 2013). Thus, a presynaptic mechanism surprisingly controls postsynaptically induced long-term synaptic plasticity.

We would like to emphasize that the selective phenotype we observed in *Nrx3*-SS4+ neurons does not mean that regulating AMPAR levels is the only function of *Nrx3*, or even of *Nrx3*-SS4 alternative splicing. It seems likely that *Nrx1*, *Nrx2*, and *Nrx3* have largely overlapping functions based on our rescue experiments (Fig. 2) and previous studies (Missler et al., 2003). Presumably, the phenotype produced by manipulating only *Nrx3* reflects neurexin functions that are incompletely compensated for by the other two neurexins, possibly because the other neurexins are not co-expressed at sufficiently high levels in the affected synapses. It seems likely that the AMPAR phenotype will be even more severe in mice carrying SS4 mutations in multiple neurexins. Moreover, alternative splicing of neurexins at SS4 may also mediate trans-synaptic control of other synaptic receptors.

How do the present results relate to previous genetic studies on α -neurexin triple KO mice, which reported changes in the presynaptic release machinery and in postsynaptic NMDARs instead of AMPARs (Kattenstroth et al., 2004; Missler et al., 2003)? It should be noted that there is not only no overlap in phenotypes, but also no overlap in genetic manipulations between the previous and the current studies. In the previous studies, all α -neurexins were deleted but β -neurexins were normally expressed, whereas in the present study, alternative splicing of both *Nrx3* α and *Nrx3* β at SS4 was selectively altered with continued unaltered expression of all α - and β -neurexins. The fact that these disparate manipulations have distinct effects supports the notion that neurexins perform multiple independent functions via different domains which are regulated by distinct events of alternative splicing. Such functional diversity is consistent with the many ligands observed for neurexins which form a complex dynamic interaction network, and emphasizes the critical role neurexins play in synaptic transmission.

Materials and Methods

In all experiments, the experimenter was blinded to the sample genotype. All plasmids are available upon requests, and the mice described here were deposited in Jackson Labs for distribution.

Mouse generation and husbandry

Nrx3^{SS4+} mutant mice were generated by homologous recombination (Fig. 1B), and *Nrx3*^{SS4-} mice were produced by cre-recombinase mediated deletion of exon 20 in the germ line of *Nrx3*^{SS4+} mutant mice (Kaeser et al., 2011). All mouse work was approved by animal use committees at Stanford (for details, see detailed methods in the SOMs).

mRNA measurements were performed using quantitative rt-PCR with β -actin as the endogenous internal control. For primer sequences and assay validations, see SOMs.

Virus preparations

All lentiviruses and AAVs were constructed as described using the synapsin promoter to drive expression (Kaeser et al., 2011). For details, see SOMs.

Hippocampal neurons were cultured from newborn WT and *Nrx3^{SS4+}* mice (Kaeser et al., 2011), infected on DIV4-5 with lentiviruses, and analyzed at DIV13-16. Rescue experiments were performed by concurrent superinfection of neurons with rescue viruses. Transfections used the calcium phosphate method.

AMPA imaging experiments were performed and quantified as described (Aoto et al., 2008; Lin et al., 2000). For details, see SOMs.

Stereotactic injections of AAVs were performed as described (Xu et al., 2012). Efficiency and localization of AAV expression was confirmed by histochemistry of nuclear GFP encoded by the expressed inactive and active GFP-Cre recombinase fusion proteins.

Electrophysiology

Recordings from cultured neurons and acute slice electrophysiology were performed essentially as described (Kaeser et al., 2011; Etherton et al., 2011; Wozny et al., 2008). For details, see SOMs.

Supplementary Material

Refer to Web version on PubMed Central for supplementary material.

Acknowledgments

We would like to thank Wei Xu, Wade Morishita, Lu Chen, and Csaba Földy for advice. This paper was supported by grants from the NIMH (R37 MH052804), the NINDS (NS077906), and the Simons Foundation (177850) to T.C.S., and by fellowship awards from the American Heart Association (11POST7360078 to J.A.) and NIDA (F32 DA031654 to D.C.M.).

References

- Aoto J, Nam CI, Poon MM, Ting P, Chen L. Synaptic signaling by all-trans retinoic acid in homeostatic synaptic plasticity. *Neuron*. 2008; 60:308–320. [PubMed: 18957222]
- Boucard AA, Chubykin AA, Comoletti D, Taylor P, Südhof TC. A splice code for trans-synaptic cell adhesion mediated by binding of neuroligin 1 to α - and β -neurexins. *Neuron*. 2005; 48:229–236. [PubMed: 16242404]
- Boucard AA, Ko J, Südhof TC. High affinity neurexin binding to cell adhesion G-protein-coupled receptor CIRL1/latrophilin-1 produces an intercellular adhesion complex. *J Biol Chem*. 2012; 287:9399–9413. [PubMed: 22262843]
- Chen YC, Lin YQ, Banerjee S, Venken K, Li J, Ismat A, Chen K, Duraine L, Bellen HJ, Bhat MA. *Drosophila* neuroligin 2 is required presynaptically and postsynaptically for proper synaptic differentiation and synaptic transmission. *J Neurosci*. 2012; 32:16018–16030. [PubMed: 23136438]
- Chih B, Gollan L, Scheiffele P. Alternative splicing controls selective trans-synaptic interactions of the neuroligin-neurexin complex. *Neuron*. 2006; 51:171–178. [PubMed: 16846852]
- Chubykin AA, Atasoy D, Etherton MR, Brose N, Kavalali ET, Gibson JR, Südhof TC. Activity-dependent validation of excitatory versus inhibitory synapses by neuroligin-1 versus neuroligin-2. *Neuron*. 2007; 54:919–931. [PubMed: 17582332]

- Comoletti D, Flynn RE, Boucard AA, Demeler B, Schirf V, Shi J, Jennings LL, Newlin HR, Südhof TC, Taylor P. Gene selection, alternative splicing, and post-translational processing regulate neuroligin selectivity for β -neurexins. *Biochemistry*. 2006; 45:12816–12827. [PubMed: 17042500]
- Craig AM, Kang Y. Neurexin-neuroligin signaling in synapse development. *Curr Opin Neurobiol*. 2007; 17:43–52. [PubMed: 17275284]
- de Wit J, Sylwestrak E, O'Sullivan ML, Otto S, Tiglio K, Savas JN, Yates JR 3rd, Comoletti D, Taylor P, Ghosh A. LRRTM2 interacts with Neurexin 1 and regulates excitatory synapse formation. *Neuron*. 2009; 64:799–806. [PubMed: 20064388]
- Etherton MR, Tabuchi K, Sharma M, Ko J, Südhof TC. An autism-associated point mutation in the neuroligin cytoplasmic tail selectively impairs AMPA receptor-mediated synaptic transmission in hippocampus. *EMBO J*. 2011; 30:2908–2919. [PubMed: 21642956]
- Heard-Costa NL, Zillikens MC, Monda KL, Johansson A, Harris TB, Fu M, Haritunians T, Feitosa MF, Aspelund T, Eiriksdottir G, et al. NRXN3 is a novel locus for waist circumference: a genome-wide association study from the CHARGE Consortium. *PLoS Genet*. 2009; 5:e1000539. [PubMed: 19557197]
- Hishimoto A, Liu QR, Drgon T, Pletnikova O, Walther D, Zhu XG, Troncoso JC, Uhl GR. Neurexin 3 polymorphisms are associated with alcohol dependence and altered expression of specific isoforms. *Hum Mol Genet*. 2007; 16:2880–2891. [PubMed: 17804423]
- Hu Z, Hom S, Kudze T, Tong XJ, Choi S, Aramuni G, Zhang W, Kaplan JM. Neurexin and neuroligin mediate retrograde synaptic inhibition in *C. elegans*. *Science*. 2012; 337:980–984. [PubMed: 22859820]
- Ichtchenko K, Hata Y, Nguyen T, Ullrich B, Missler M, Moomaw C, Südhof TC. Neuroligin 1: a splice site-specific ligand for β -neurexins. *Cell*. 1995; 81:435–443. [PubMed: 7736595]
- Iijima T, Wu K, Witte H, Hanno-Iijima Y, Glatter T, Richard S, Scheiffele P. SAM68 regulates neuronal activity-dependent alternative splicing of neurexin-1. *Cell*. 2011; 147:1601–1614. [PubMed: 22196734]
- Kaaser PS, Deng L, Wang Y, Dulubova I, Liu X, Rizo J, Südhof TC. RIM proteins tether Ca^{2+} channels to presynaptic active zones via a direct PDZ-domain interaction. *Cell*. 2011; 144:282–295. [PubMed: 21241895]
- Kattenstroth G, Tantalaki E, Südhof TC, Gottmann K, Missler M. Postsynaptic N-methyl-D-aspartate receptor function requires α -neurexins. *Proc Natl Acad Sci U S A*. 2004; 101:2607–2612. [PubMed: 14983056]
- Kerchner GA, Nicoll RA. Silent synapses and the emergence of a postsynaptic mechanism for LTP. *Nat Rev Neurosci*. 2008; 9:813–825. [PubMed: 18854855]
- Ko J, Fuccillo MV, Malenka RC, Südhof TC. LRRTM2 functions as a neurexin ligand in promoting excitatory synapse formation. *Neuron*. 2009; 64:791–798. [PubMed: 20064387]
- Koester HJ, Johnston D. Target cell-dependent normalization of transmitter release at neocortical synapses. *Science*. 2005; 308:863–866. [PubMed: 15774725]
- Krueger DD, Tuffy LP, Papadopoulos T, Brose N. The role of neurexins and neuroligins in the formation, maturation, and function of vertebrate synapses. *Curr Opin Neurobiol*. 2012; 22:412–422. [PubMed: 22424845]
- Lachman HM, Fann CS, Bartzis M, Evgrafov OV, Rosenthal RN, Nunes EV, Miner C, Santana M, Gaffney J, Riddick A, et al. Genomewide suggestive linkage of opioid dependence to chromosome 14q. *Hum Mol Genet*. 2007; 16:1327–1334. [PubMed: 17409192]
- Lee K, Kim Y, Lee SJ, Qiang Y, Lee D, Lee HW, Kim H, Je HS, Südhof TC, Ko J. MDGAs interact selectively with neuroligin-2 but not other neuroligins to regulate inhibitory synapse development. *Proc Natl Acad Sci U S A*. 2013; 110:336–341. [PubMed: 23248271]
- Lin JW, Ju W, Foster K, Lee SH, Ahmadian G, Wyszynski M, Wang YT, Sheng M. Distinct molecular mechanisms and divergent endocytotic pathways of AMPA receptor internalization. *Nat Neurosci*. 2000; 3:1282–1290. [PubMed: 11100149]
- Matsuda K, Yuzaki M. Cbln family proteins promote synapse formation by regulating distinct neurexin signaling pathways in various brain regions. *Eur J Neurosci*. 2011; 33:1447–1461. [PubMed: 21410790]

- Menendez de la Prida L, Suarez F, Pozo MA. Electrophysiological and morphological diversity of neurons from the rat subicular complex in vitro. *Hippocampus*. 2003; 13:728–744. [PubMed: 12962317]
- Missler M, Zhang W, Rohlmann A, Kattenstroth G, Hammer RE, Gottmann K, Südhof TC. α -Neurexins couple Ca^{2+} channels to synaptic vesicle exocytosis. *Nature*. 2003; 423:939–948. [PubMed: 12827191]
- O'Mara S. The subiculum: what it does, what it might do, and what neuroanatomy has yet to tell us. *J Anat*. 2005; 207:271–282. [PubMed: 16185252]
- Resnick M, Segall A, G GR, Lupowitz Z, Zisapel N. Alternative splicing of neurexins: a role for neuronal polypyrimidine tract binding protein. *Neurosci Lett*. 2008; 439:235–240. [PubMed: 18534753]
- Reichelt AC, Rodgers RJ, Clapcote SJ. The role of neurexins in schizophrenia and autistic spectrum disorder. *Neuropharmacology*. 2012; 62:1519–1526. [PubMed: 21262241]
- Reyes A, Lujan R, Rozov A, Burnashev N, Somogyi P, Sakmann B. Target-cell-specific facilitation and depression in neocortical circuits. *Nat Neurosci*. 1998; 1:279–285. [PubMed: 10195160]
- Rowen L, Young J, Birditt B, Kaur A, Madan A, Philipps DL, Qin S, Minx P, Wilson RK, Hood L, et al. Analysis of the human neurexin genes: alternative splicing and the generation of protein diversity. *Genomics*. 2002; 79:587–597. [PubMed: 11944992]
- Rozic G, Lupowitz Z, Zisapel N. Exonal Elements and Factors Involved in the Depolarization-Induced Alternative Splicing of Neurexin 2. *J Mol Neurosci*. 2012
- Schnell E, Bensen AL, Washburn EK, Westbrook GL. Neuroligin-1 overexpression in newborn granule cells in vivo. *PLoS One*. 2012; 7:e48045. [PubMed: 23110172]
- Schwenk J, Harmel N, Brechet A, Zolles G, Berkefeld H, Müller CS, Bildl W, Baehrens D, Huber B, Kulik A, et al. High-resolution proteomics unravel architecture and molecular diversity of native AMPA receptor complexes. *Neuron*. 2012; 74:621–633. [PubMed: 22632720]
- Shapiro-Reznik M, Jilg A, Lerner H, Earnest DJ, Zisapel N. Diurnal rhythms in neurexins transcripts and inhibitory/excitatory synapse scaffold proteins in the biological clock. *PLoS One*. 2012; 7:e37894. [PubMed: 22662246]
- Siddiqui TJ, Pancaroglu R, Kang Y, Rooyakkers A, Craig AM. LRRTMs and neuroligins bind neurexins with a differential code to cooperate in glutamate synapse development. *J Neurosci*. 2010; 30:7495–7506. [PubMed: 20519524]
- Soler-Llavina GJ, Fuccillo MV, Ko J, Südhof TC, Malenka RC. The neurexin ligands, neuroligins and leucine-rich repeat transmembrane proteins, perform convergent and divergent synaptic functions in vivo. *Proc Natl Acad Sci U S A*. 2011; 108:16502–16509. [PubMed: 21953696]
- Soler-Llavina GJ, Arstikaitis P, Morishita W, Ahmad M, Südhof TC, Malenka RC. Leucine-Rich Repeat Transmembrane Proteins Are Essential for Maintenance of Long-term Potentiation. *Neuron*. 2013 in press.
- Staff NP, Jung HY, Thiagarajan T, Yao M, Spruston N. Resting and active properties of pyramidal neurons in subiculum and CA1 of rat hippocampus. *J Neurophysiol*. 2000; 84:2398–2408. [PubMed: 11067982]
- Südhof TC. Neuroligins and neurexins link synaptic function to cognitive disease. *Nature*. 2008; 455:903–911. [PubMed: 18923512]
- Sugita S, Khvochtev M, Südhof TC. Neurexins are functional α -latrotoxin receptors. *Neuron*. 1999; 22:489–496. [PubMed: 10197529]
- Sugita S, Saito F, Tang J, Satz J, Campbell K, Südhof TC. A stoichiometric complex of neurexins and dystroglycan in brain. *J Cell Biol*. 2001; 154:435–445. [PubMed: 11470830]
- Tabuchi K, Südhof TC. Structure and evolution of neurexin genes: insight into the mechanism of alternative splicing. *Genomics*. 2002; 79:849–859. [PubMed: 12036300]
- Taniguchi H, Gollan L, Scholl FG, Mahadomrongkul V, Dobler E, Limthong N, Peck M, Aoki C, Scheiffele P. Silencing of neuroligin function by postsynaptic neurexins. *J Neurosci*. 2007; 27:2815–2824. [PubMed: 17360903]
- Taube JS. Electrophysiological properties of neurons in the rat subiculum in vitro. *Exp Brain Res*. 1993; 96:304–318. [PubMed: 7903643]

- Uemura T, Lee SJ, Yasumura M, Takeuchi T, Yoshida T, Ra M, Taguchi R, Sakimura K, Mishina M. Trans-synaptic interaction of GluRdelta2 and Neurexin through Cbln1 mediates synapse formation in the cerebellum. *Cell*. 2010; 141:1068–1079. [PubMed: 20537373]
- Ullrich B, Ushkaryov YA, Südhof TC. Cartography of neurexins: more than 1000 isoforms generated by alternative splicing and expressed in distinct subsets of neurons. *Neuron*. 1995; 14:497–507. [PubMed: 7695896]
- Ushkaryov YA, Hata Y, Ichtchenko K, Moomaw C, Afendis S, Slaughter CA, Südhof TC. Conserved domain structure of β -neurexins. Unusual cleaved signal sequences in receptor-like neuronal cell-surface proteins. *J Biol Chem*. 1994; 269:11987–11992. [PubMed: 8163501]
- Ushkaryov YA, Petrenko AG, Geppert M, Südhof TC. Neurexins: synaptic cell surface proteins related to the α -latrotoxin receptor and laminin. *Science*. 1992; 257:50–56. [PubMed: 1621094]
- Ushkaryov YA, Südhof TC. Neurexin III α : extensive alternative splicing generates membrane-bound and soluble forms. *Proc Natl Acad Sci U S A*. 1993; 90:6410–6414. [PubMed: 8341647]
- Vaags AK, Lionel AC, Sato D, Goodenberger M, Stein QP, Curran S, Ogilvie C, Ahn JW, Drmic I, Senman L, et al. Rare deletions at the neurexin 3 locus in autism spectrum disorder. *Am J Hum Genet*. 2012; 90:133–141. [PubMed: 22209245]
- Wozny C, Maier N, Schmitz D, Behr J. Two different forms of long-term potentiation at CA1-subiculum synapses. *J Physiol*. 2008; 586:2725–2734. [PubMed: 18403426]
- Xu W, Morishita W, Buckmaster PS, Pang ZP, Malenka RC, Südhof TC. Distinct neuronal coding schemes in memory revealed by selective erasure of fast synchronous synaptic transmission. *Neuron*. 2012; 73:990–1001. [PubMed: 22405208]

Highlights

- Conditional knockin controls neurexin alternative splicing at a single site
- Presynaptic neurexin alternative splicing regulates postsynaptic AMPA-receptors
- Alternative splicing of neurexin selectively controls AMPA-receptor trafficking
- Postsynaptic NMDAR-dependent LTP requires presynaptic neurexin alternative splicing

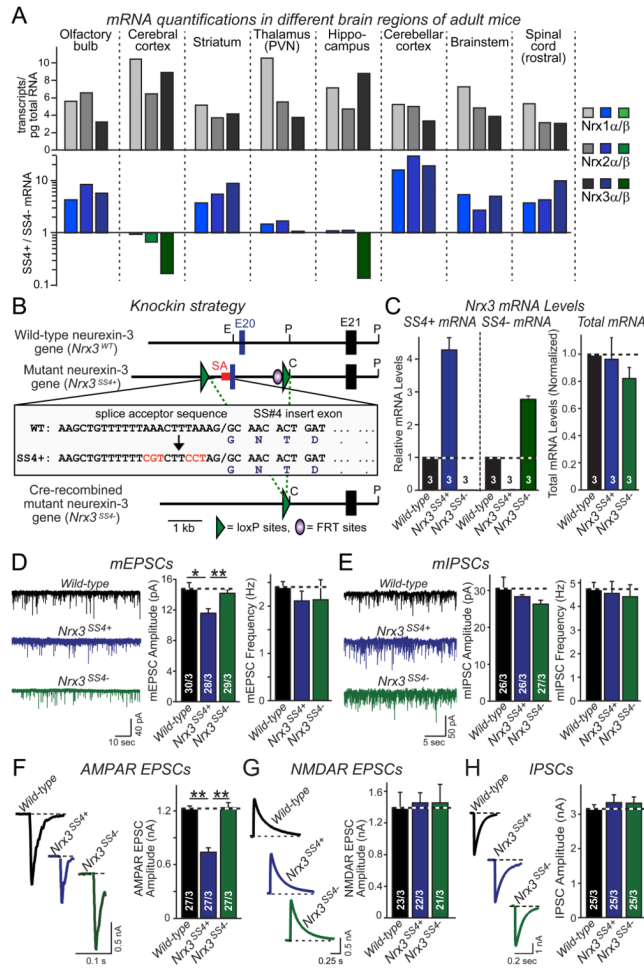


Figure 1. Genetic switching of alternative splicing of Nr3 at SS4 into constitutive ‘on’ or ‘off’ states alters AMPAR-mediated synaptic transmission

A. Absolute expression (# transcripts/pg total RNA) of Nr3 α/β , Nr2 α/β , and Nr3 α/β mRNAs in the indicated brain regions (top), and relative levels of SS4+ and SS4- mRNAs in the same brain regions as determined by quantitative rt-PCR (bottom; n = 4 mice; PVN, paraventricular nucleus).

B. Knock-in strategy to generate conditional Nr3-SS4 mutant mice. The imperfect splice acceptor sequence (SA; sequence in inset) of the alternatively spliced SS4 exon 20 (E20) was replaced by homologous recombination in murine ES cells with a perfect splice acceptor sequence (red letters); in addition, exon 20 was flanked by LoxP sites. The resulting mutant Nr3 gene constitutively expresses Nr3-SS4+ mRNA (*Nrx3*^{SS4+}). Cre-recombinase deletes the exon, causing constitutive expression of Nr3-SS4- mRNA (*Nrx3*^{SS4-}). Single letters indicate locations of restriction enzyme sites (C, ClaI; E, EcoRI; P, PstI).

C. Quantification of Nr3-SS4+, Nr3-SS4-, and total Nr3 mRNA levels in hippocampal neurons cultured from WT or *Nrx3*^{SS4+} mice; *Nrx3*^{SS4+} neurons were infected with lentiviruses expressing inactive cre-recombinase (retaining the *Nrx3*^{SS4+} genotype) or active cre-recombinase (converting *Nrx3*^{SS4+} into *Nrx3*^{SS4-} neurons). mRNA levels were normalized to those observed in WT neurons which express predominantly Nr3-SS4- mRNA (see panel A; n=3 independent cultures).

D & E. Representative traces (left) and summary graphs of the amplitude and frequency (right) of mEPSCs (D) and mIPSCs (E), monitored in cultured hippocampal WT, *Nrx3*^{SS4+}, and *Nrx3*^{SS4-} neurons obtained as described for C.

F-H. Representative traces (left) and summary graphs (right) of evoked AMPAR- (F) and NMDAR-mediated EPSCs (G) and of evoked IPSCs (H) in cultured hippocampal WT, *Nrx3*^{SS4+} and *Nrx3*^{SS4-} neurons.

Data in C-H are means \pm SEM; numbers in bars give number of independent experiments (C) or number of total cells/independent experiments analyzed (D-H). For D-H, statistical significance was calculated by single-factor ANOVA (** $p < 0.01$). See also Fig. S1.

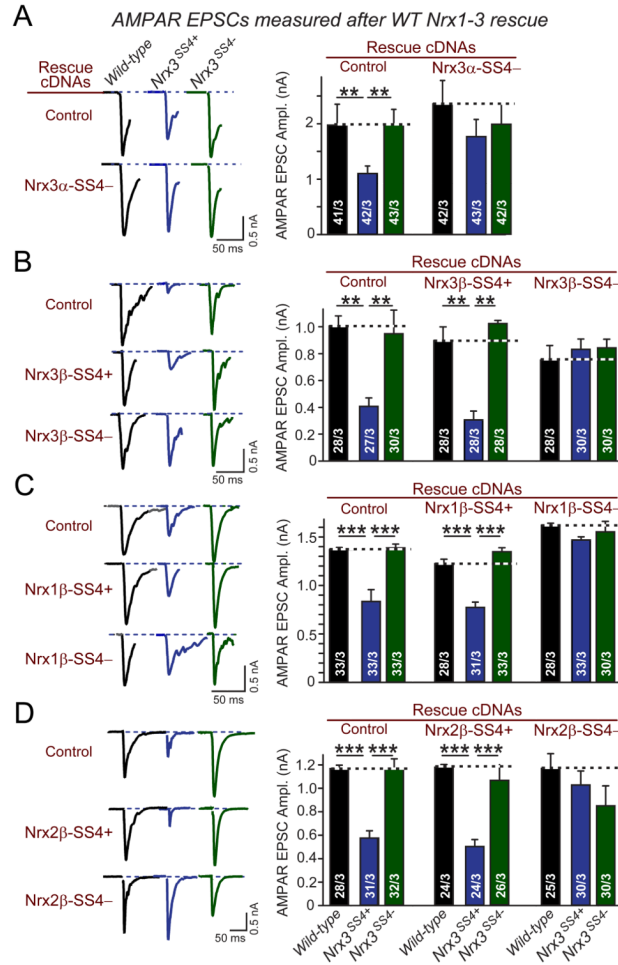


Figure 2. Reduced AMPAR-mediated synaptic responses in *Nrx3^{SS4+}* synapses are rescued by *SS4-* but not *SS4+* neurexins

A-D. Representative traces (left) and summary graphs (right) of evoked AMPAR-mediated peak EPSC amplitudes measured in hippocampal neurons that were cultured from WT or *Nrx3^{SS4+}* mice; *Nrx3^{SS4+}* neurons were infected with lentiviruses expressing inactive cre-recombinase (which leaves the genotype unchanged) or active cre-recombinase (which converts the *Nrx3^{SS4+}* into the *Nrx3^{SS4-}* genotype). Neurons were superinfected with a second lentivirus expressing either no neurexin (Control) or the indicated *Nrx1-3* isoforms and splice variants.

Data are means \pm SEM; numbers in bars represent total number of cells/experiments analyzed. Statistical significance was calculated by single-factor ANOVA (*, $p < 0.05$; **, $p < 0.01$; ***, $p < 0.001$).

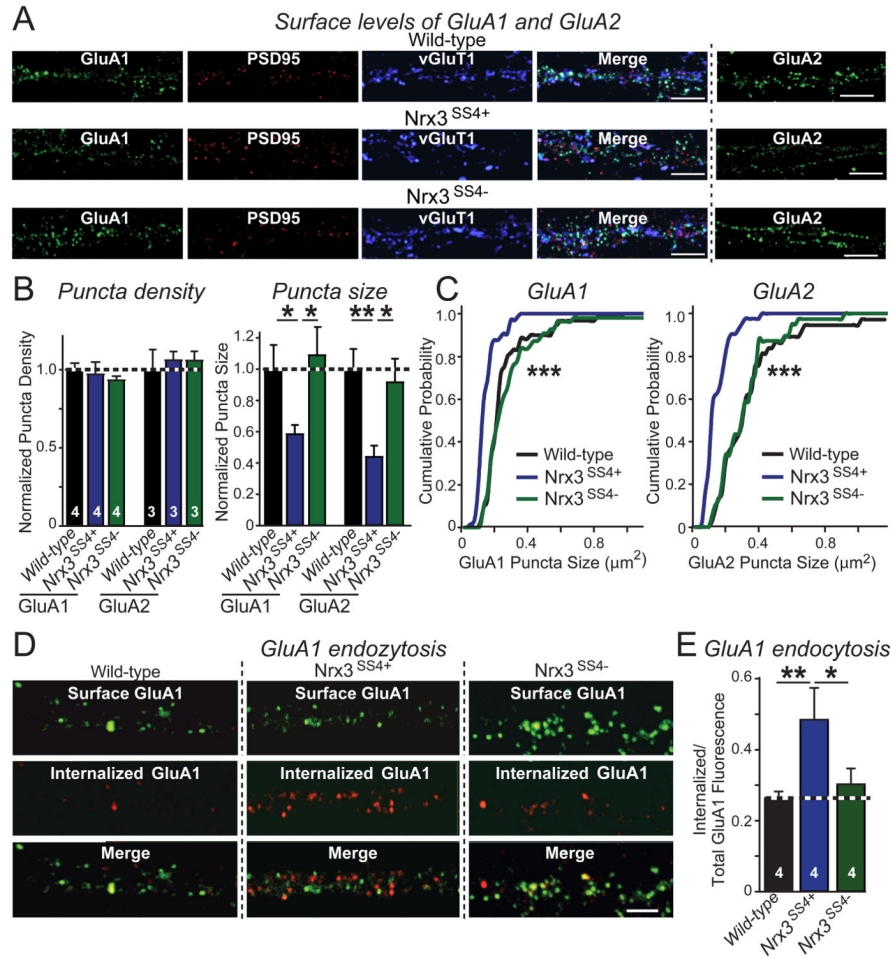


Figure 3. GluA1 and GluA2 AMPAR surface levels are reduced in hippocampal Nr3^{SS4+} neurons due to increased internalization

A. Representative images of hippocampal neurons cultured from WT or Nr3^{SS4+} mice; Nr3^{SS4+} neurons were infected with lentiviruses expressing either inactive (retaining the Nr3^{SS4+} genotype) or active cre-recombinase (switching the Nr3^{SS4+} to the Nr3^{SS4-} genotype). Neurons were surface-labeled for GluA1 or GluA2 AMPARs (see Fig. S2A for experimental protocol); GluA1-stained neurons were permeabilized and also stained for the excitatory synaptic markers PSD95 and vGluT1 (green: surface GluA1; red: PSD95; blue: vGluT1; scale bars, 5 μm).

B. Quantifications of the normalized density and size of synaptic puncta labeled for surface GluA1 or GluA2 in WT, Nr3^{SS4+}, or Nr3^{SS4-} neurons. For more data, see Figs. S2B and S2C.

C. Cumulative distributions of Nr3^{SS4+} and Nr3^{SS4-} GluA1 and GluA2 puncta sizes.

D & E. Representative images (D) and summary graph (E) of GluA1 endocytosis analyzed in WT, Nr3^{SS4+}, and Nr3^{SS4-} neurons obtained as described above. GluA1 endocytosis was quantified by dividing the internalized GluA1 fraction (red) by the total GluA1 signal (surface fraction (green) + internalized fraction (red)); scale bar, 5 μm ; see Fig. S2D).

Data are the means \pm SEM of 4 independent experiments. Statistical analyses were performed by single-factor ANOVA (* $p < 0.05$; ** $p < 0.01$; *** $p < 0.001$).

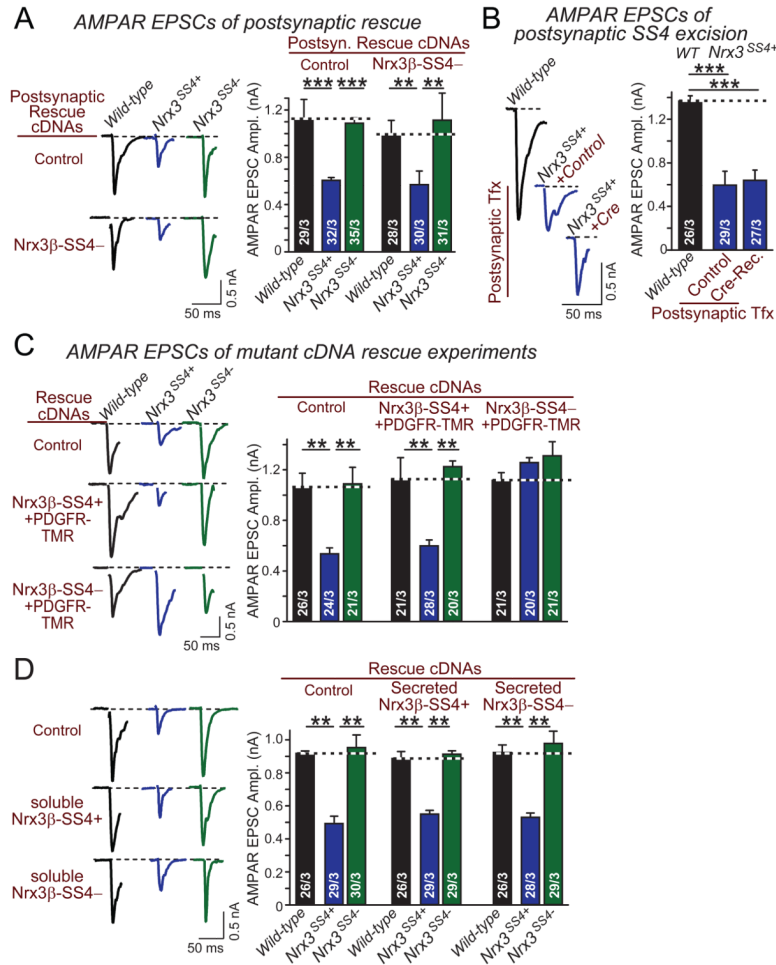


Figure 4. Presynaptic membrane-tethered but not secreted Nr3β-SS4- controls post-synaptic AMPARs in a non cell-autonomous fashion

A. Representative traces (left) and summary graphs (right) of evoked AMPAR EPSCs monitored in hippocampal neurons cultured from WT or *Nrx3^{SS4+}* mice. *Nrx3^{SS4+}* neurons were sparsely transfected at DIV4-5 with plasmids encoding EGFP alone or EGFP and Nr3β-SS4-, and were analyzed by whole-cell patch-clamp recordings at DIV14-16.

B. Same as A, except that neurons were sparsely transfected with plasmids encoding inactive (Control) or active cre-recombinase (Cre-Rec).

C. Representative traces (left) and summary graphs of AMPAR-mediated EPSC amplitudes in hippocampal neurons that were cultured from WT or *Nrx3^{SS4+}* mice, and infected with lentiviruses expressing inactive cre-recombinase (which retains the *Nrx3^{SS4+}* genotype) or active cre-recombinase (which converts *Nrx3^{SS4+}* into *Nrx3^{SS4-}* neurons). Neurons were superinfected with lentivirus expressing control or rescue cDNAs encoding fusion proteins of the extracellular Nr3β-SS4+ and -SS4- sequences with the PDGF-receptor transmembrane region.

D. Same as C, except that the rescue cDNAs express a naturally occurring splice variant of Nr3β that encodes secreted Nr3β-SS4+ and Nr3β-SS4-.

Data are means ± SEM; numbers in bars represent total cells/experiments performed. Statistical significance was calculated by single-factor ANOVA (** p<0.01; *** p<0.001).

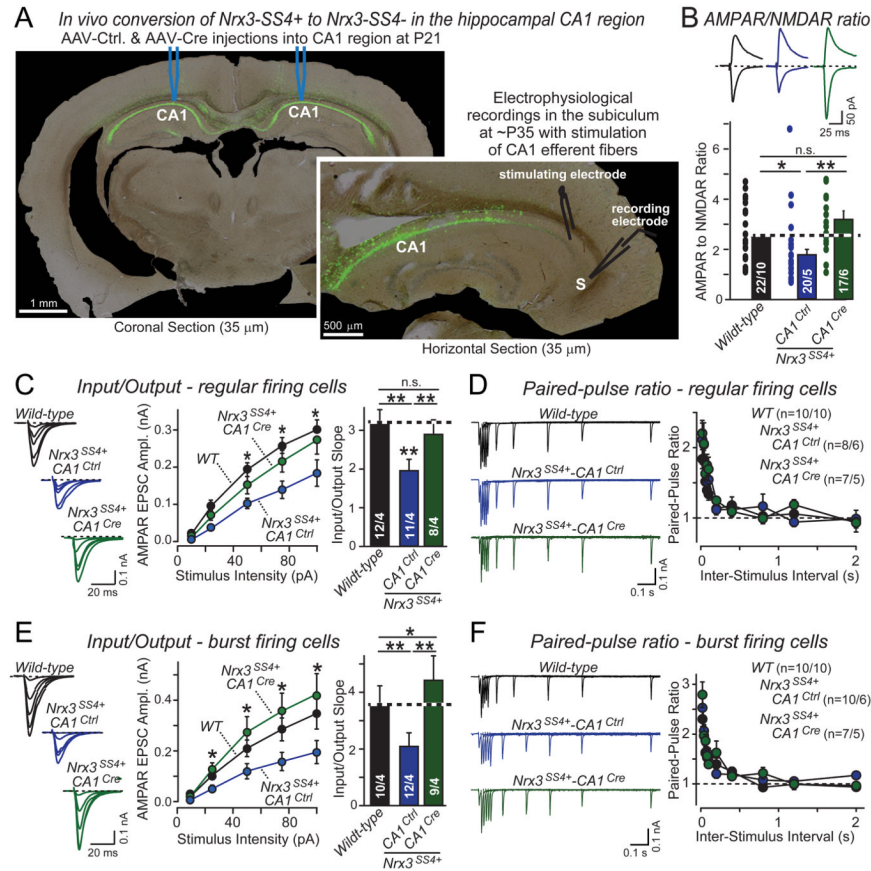


Figure 5. Cre-mediated *in vivo* conversion of presynaptic *Nrx3*^{SS4+} to *Nrx3*^{SS4-} in the hippocampal CA1 region restores impaired AMPAR-mediated synaptic responses in *Nrx3*^{SS4+} postsynaptic neurons in the subiculum

A. Representative images illustrating the selective expression of EGFP in the CA1 region of the dorsal hippocampus after stereotactic injection of AAVs and the recording configuration used for measuring synaptic transmission from the CA1 region to the subiculum. Mice were stereotactically injected at P21, and analyzed at P35. Note the complete infection of CA1 region neurons without spillover into the subiculum (S).

B. AMPAR/NMDAR ratios recorded in acute slices in pyramidal neurons of the subiculum after *in vivo* presynaptic manipulations of *Nrx3*-SS4 alternative splicing in the hippocampal CA1 region (top, representative EPSC traces at -65 mV [AMPA] and +40 mV [NMDA]; bottom, average ratios). WT mice were stereotactically injected into the hippocampal CA1 region with AAVs encoding GFP (black traces/bars), and *Nrx3*^{SS4+} mutant mice with AAVs encoding inactive (*Nrx3*^{SS4+}-CA1 Ctrl; blue traces/bars) or active cre-recombinase (*Nrx3*^{SS4+}-CA1 Cre; green traces/bars).

C. Input/output relationship of postsynaptic AMPAR EPSCs in regular firing neurons of the subiculum as a function of presynaptic *Nrx3*-SS4 alternative splicing. Data show sample traces (left), summary curves (middle), and average input/output slopes (right) for slices obtained as described in B.

D. Paired-pulse measurements of postsynaptic AMPAR EPSCs in regular firing neurons of the subiculum as a function of presynaptic *Nrx3*-SS4 alternative splicing. Data show sample traces (left) and summary graphs (right) for samples obtained as described in B.

E & F. Same as C and D, but recorded from burst-firing neurons in the subiculum.

Data shown are means \pm SEM; number number of neurons/mice analyzed are shown in the bars. Statistical analyses for summary graphs were performed by single-factor ANOVA (*, $p < 0.05$; **, $p < 0.01$). For more data, see Fig. S3.

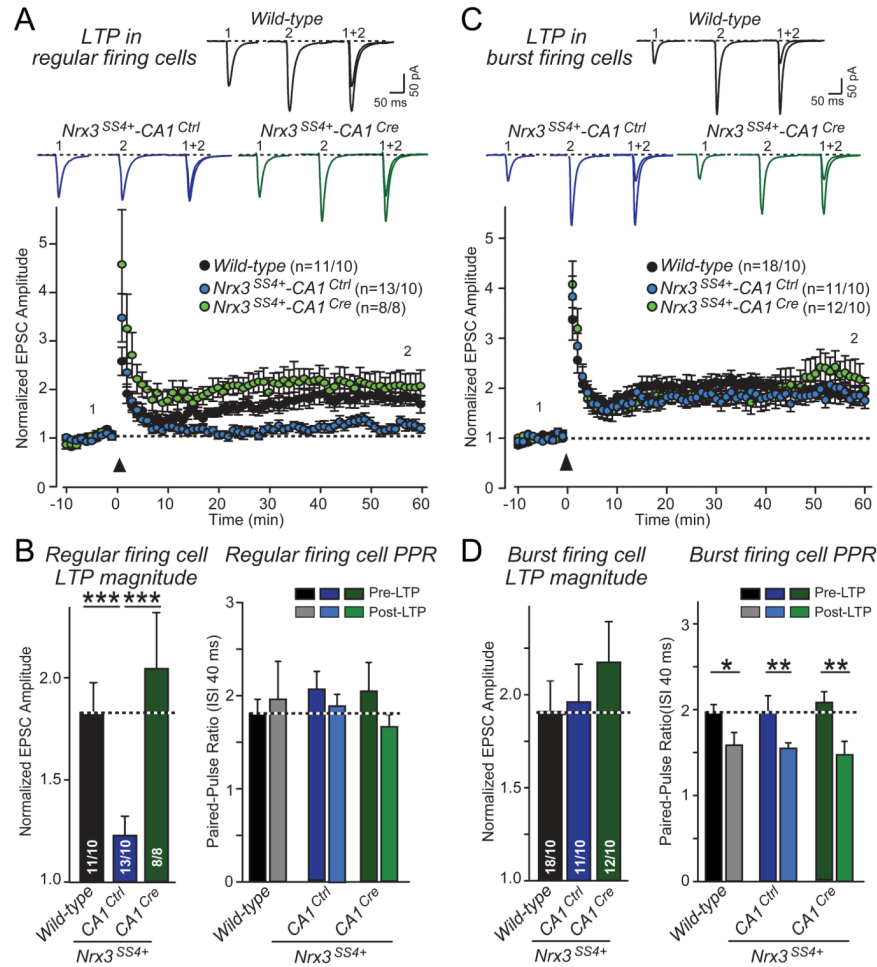


Figure 6. *Nrx3^{SS4+}* mice exhibit impaired postsynaptic NMDAR-dependent LTP that is rescued by conversion of presynaptic *Nrx3^{SS4+}* neurons into *Nrx3^{SS4-}* neurons

A. LTP in regular firing neurons. Acute slices were analyzed by whole-cell recordings in the subiculum from WT mice and from *Nrx3^{SS4+}* mice in which CA1 neurons were transduced *in vivo* by stereotactic injection of AAV encoding inactive (Ctrl) or active cre-recombinase (Cre). Data show representative traces (top) and summary graphs of the relative synaptic strength (bottom) monitored before and after induction of LTP. LTP was induced by 4×100 Hz stimuli applied for 1 sec with 10 sec intervals in current clamp configuration at resting membrane potential. Following the LTP induction, cells were held at -65 mV in voltage-clamp to measure evoked EPSCs. Representative traces shown are EPSCs during baseline (1) and 50 minutes after induction (2).

B. EPSC amplitudes averaged over the last 10 min of the LTP recordings, normalized to the baseline (left), and paired-pulse ratios with a 40 ms inter-stimulus interval measured 10 min pre-LTP induction and 60 min post-LTP induction (right) from regular firing neurons in the subiculum following presynaptic manipulation of *Nrx3-SS4*.

C & D. Same as A and B, but for burst firing neurons in the subiculum. Note that consistent with previous studies (Wozny et al., 2008), LTP in burst firing neurons causes a change in paired-pulse ratio suggesting it is presynaptic (D), whereas LTP in regular firing neurons does not cause a change in paired-pulse ratio consistent with a postsynaptic localization (B). Data shown are means \pm SEM; numbers of neurons/mice examined are shown in the graphs. Statistical analyses were performed by single-factor ANOVA (* $p < 0.05$; ** $p < 0.01$; *** $p < 0.001$). See also Fig. S4.

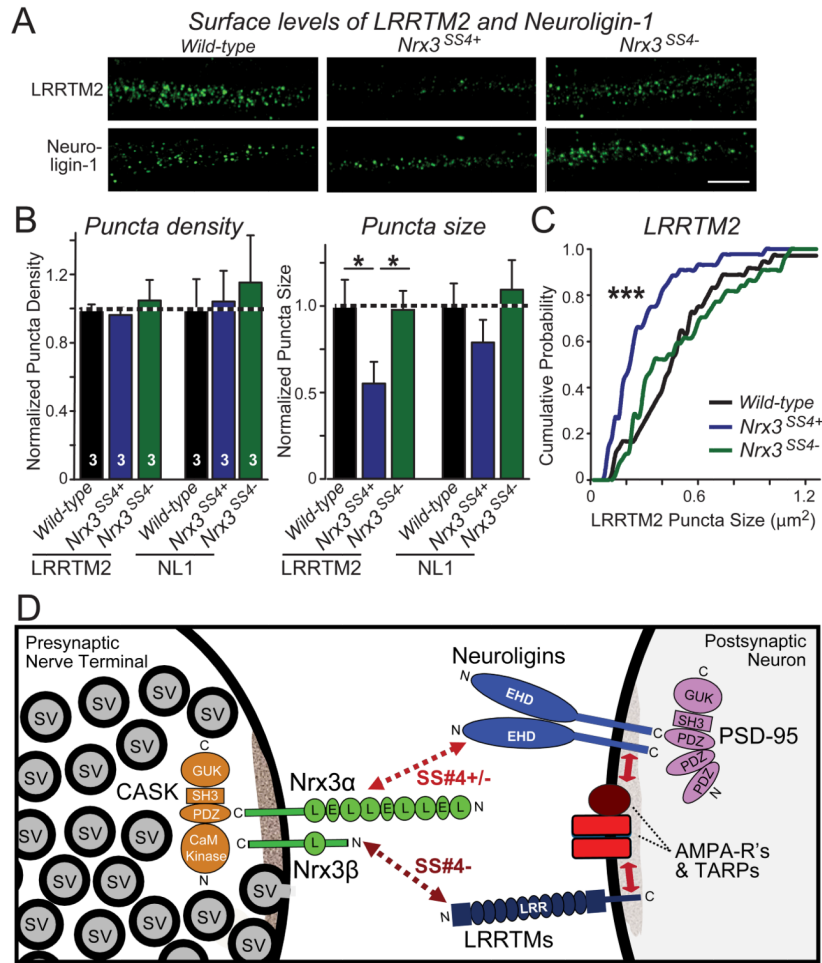


Figure 7. *Nrx3^{SS4+}* neurons contain decreased postsynaptic concentrations of LRRTM2: Model for the mechanism of action of *Nrx3*-*SS4* alternative splicing

A. Representative images of hippocampal neurons stained for surface-localized LRRTM2 or neuroigin-1 (NL1). Neurons were cultured from WT or *Nrx3^{SS4+}* mice; the latter were infected with lentiviruses expressing either inactive cre-recombinase (which retains the *Nrx3^{SS4+}* genotype) or active cre-recombinase (which switches *Nrx3^{SS4+}* into *Nrx3^{SS4-}* neurons).

B. Quantification of the density (left) and size (right) of LRRTM2 or neuroigin-1 positive puncta in WT, *Nrx3^{SS4+}*, and *Nrx3^{SS4-}* neurons. Data are means \pm SEM; n=3 independent culture experiments; statistical analyses were performed by Student's t-test (*, p<0.05).

C. Cumulative probability distribution of the puncta size in WT, *Nrx3^{SS4+}*, and *Nrx3^{SS4-}* neurons. Statistical significance was assessed by the Kolmogorov-Smirnov test (***, p<0.001). See also Fig. S5.

D. Model of how presynaptic *Nrx3* may stabilize postsynaptic AMPARs in an *SS4*-dependent manner via trans-synaptic interactions with neuroigin-1 and/or LRRTMs. Postsynaptic AMPAR stability is dependent on the presynaptic expression of *Nrx3*-*SS4*—that lacks an insert at splice site 4, and preferentially interacts with neuroiginins and LRRTMs. Neuroiginins and LRRTMs have been shown to interact with AMPARs (Etherton et al., 2011; Soler-Llavina et al., 2011; Schwenk et al., 2012), possibly via their binding to PSD95 which in turn binds to the C-terminal sequences of TARPs that form a tight complex with AMPARs (Schnell et al., 2002). The data in panels A-C suggest that the *Nrx3*-LRRTM interaction is most important for controlling postsynaptic AMPAR levels, but different

isoforms of neuroligin differentially interact with the two Nr3-SS4 splice variants, and thus a major contribution of the Nr3-neuroligin interaction in controlling postsynaptic AMPARs cannot be ruled out.